Chain-Length Anomaly in the Two-Dimensional Ordering of the Cationic Surfactants C_nTAB at the Graphite/Water Interface, Revealed by Advanced Calorimetric Methods

Zoltán Király,*,†,‡ Gerhard H. Findenegg,‡ and Ágnes Mastalir§

Department of Colloid Chemistry, University of Szeged, Aradi Vt. 1, H-6720 Szeged, Hungary; Stranski-Laboratory for Physical and Theoretical Chemistry, Technical University of Berlin, Strasse des 17. Juni 112, D-10623 Berlin, Germany; and Department of Organic Chemistry, University of Szeged, Dóm tér 8, H-6720 Szeged, Hungary

Received: May 27, 2003; In Final Form: September 16, 2003

Surfactants adsorbed at the graphite/aqueous solution interface form half-cylindrical surface micelles templated by a flat, ordered monolayer. Here, the differential heats of adsorption of even-numbered alkyltrimethylammonium bromides C_nTAB ($n = 6-16$) were measured in the monolayer region by frontal-flow calorimetry and pulsed-flow calorimetry. The monolayer self-assembles exothermically and with a negative change of heat capacity. Pure water and pure surfactant domains coexist in the submonolayer region. The differential heat of adsorption is independent of the surface coverage and increases linearly with n, but a step occurs between $n = 10$ and $n = 12$. The adsorption is reversible below this critical chain length, but is nonreversible above it. This anomaly has been interpreted in terms of a reorientation of the headgroup from nonbonding to bonding with respect to the surface, and the formation of two different two-dimensional crystal structures on the surface. Pulsed-flow calorimetry, ideally suited for the study of nonreversible adsorption processes, has a high potential for the investigation of a variety of solid/liquid interfacial phenomena that cannot be studied by other current calorimetric methods.

Introduction

The visualization of solid/nonaqueous solution interfaces by scanning tunneling microscopy (STM) revealed that long-chain alkane molecules, alcohols, fatty acids, alkyl halides, and other related compounds form highly ordered two-dimensional (2D) layers on the surface of graphite.[1,2] In a close-packed monolayer, the adsorbed molecules lie flat on the surface in their extended trans conformation, packed parallel to each other and in a head-to-head, tail-to-tail arrangement. The calorimetric enthalpies of adsorption correlate well with the STM images on the same and related systems, and provide further insight into the thermodynamic aspects of surface-directed ordering.[3,4] The lattice fit between the graphite hexagons and the alkyl chains causes strong attractive interactions of the paraffinic molecules with the hydrophobic surface of graphite. The high stability of the monolayer is increased by lateral interactions between neighboring molecules, which, in turn, are further influenced by the temperature, the length of the carbon skeleton, and the nature of the headgroup.

Atomic force microscopy (AFM) studies indicated that anionic,[5] cationic,[6−10] and nonionic[10−13] surfactants adsorbed at the graphite/aqueous solution interface form half-cylindrical surface micelles templated by an ordered monolayer. Surface-directed ordering was claimed to be governed by a directional anisotropy in van der Waals interactions, rather than epitaxy, between the tailgroup and the surface lattice.[6−8] Calorimetric studies demonstrated that such monolayer formation is strongly exothermic and, for a number of cases, effectively irreversible.[14−18] In contrast, surface-induced hemimicellization is always reversible. The process is moderately exothermic for anionic[14] and cationic[15] surfactants, and endothermic for nonionics.[16−18]

A combination of STM and AFM studies at the molecular level with adsorption calorimetry at the thermodynamic level offers a most promising way to investigate the adsorption of aliphatic compounds at solid/solution interfaces. However, STM is not applicable under aqueous conditions and the current AFM methods are not suitable for patterning surfaces in the submonolayer region, at equilibrium concentrations far below the critical micelle concentration. The high-affinity adsorption of surfactants at the graphite/water interface is challenging; only integral molar heats rather than differential molar heats have been measured calorimetrically, with poor resolution, if any, of the monolayer regime.

Flow sorption microcalorimetry was invented and progressively developed by Groszek.[19,20] We recently reported on an automated flow sorption/microcalorimeter system designed for simultaneous measurements of the material balance and the enthalpy balance of adsorption at solid/solution interfaces[15,18] in order to measure differential heats of adsorption with higher accuracy as compared with those calculated from a combination of separately measured adsorption and enthalpy isotherms. We report here on a calorimetric study of the adsorption in the submonolayer region of a series of cationic surfactants (even-numbered alkyltrimethylammonium bromides, from C_6TAB to C_{16}TAB) from aqueous solutions onto graphite. The differential enthalpies of adsorption were determined as functions of the surface coverage and the temperature.

Experimental Section

C_nTABr *n*-alkyltrimethylammonium bromides with $n = 6$ (98%, Lancaster), 8 and 10 (98%, Fluka), 12 and 16 (99%,

* To whom correspondence should be addressed. E-mail: zkiraly@chem.u-szeged.hu.
† Department of Colloid Chemistry, University of Szeged.
‡ Stranski-Laboratory for Physical and Theoretical Chemistry, TU Berlin.
§ Department of Organic Chemistry, University of Szeged.

10.1021/jp035466t CCC: $25.00
Published on Web 10/18/2003

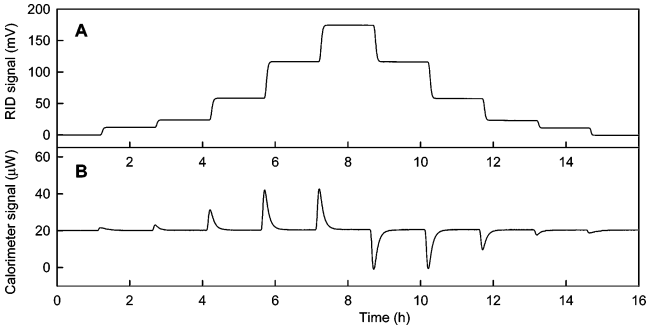

Figure 1. Frontal-flow experiment. (A) RID signal and (B) calorimeter signal of the step-by-step adsorption of C_6TAB from aqueous solutions onto graphite at 298.15 K. Column packing 188.3 mg of V3G; flow rate 11.17 cm^3/h; concentration sequence 0, 0.5, 1.0, 2.5, 5.0, and 7.5 $mmol/dm^3$. Adsorption steps are followed by desorption steps. Monolayer formation is seen to be reversible.

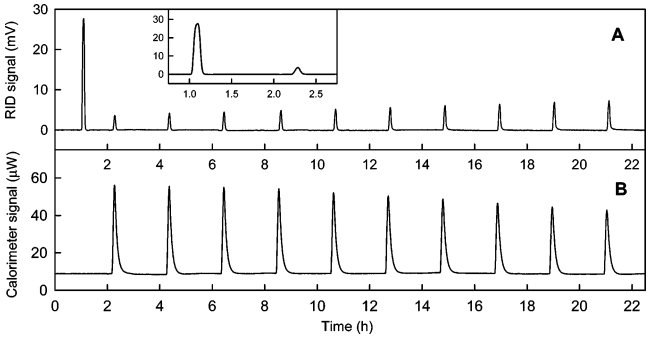

Figure 2. Pulsed-flow experiment. (A) RID signal and (B) calorimeter signal of the successive saturation of the graphite surface with C_{16}-TAB from water at 298.15 K. Column packing 43.2 mg of V3G; water flow rate 11.75 cm^3/h; pulse concentration 0.4 $mmol/dm^3$; pulse volume 0.980 cm^3. The first RID peak is representative of the input pulses. Subsequent peaks are output pulses. Monolayer formation is seen to be nonreversible.

Sigma), and 14 (99%, Aldrich) were used as received. Reagent-grade water was produced by a Milli-Q filtration system. The graphite sample, V3G (Vulcan3, a carbon black by Cabot Corp., USA, graphitized by Sigri Elektrographite GmbH, Meitingen, Germany), had a BET surface area to N_2 of 68 m^2/g at 77 K.

The automated measuring system consisted of a TAM 2277 isotherm microcalorimeter (ThermoMetrics, Lund, Sweden) and an auxiliary HPLC device (a high-performance liquid chromatograph) supplied with a differential refractive index detector, RID (Knauer, Berlin, Germany).[15,18] Typically, 0.04−0.2 g of V3G was weighed in a small chromatographic column and placed inside the measuring block of the calorimeter. The HPLC system was used to control the liquid flow (6−12 $cm^3 \cdot h^{-1}$), to change the solutions entering the column, and to monitor the concentration waves (in terms of refractive index variation) passing through the column. Measurements were made at the set temperature $\pm 2 \times 10^{-4}$ K.

Results

Frontal-Flow Calorimetry. The calorimeter vessel was loaded with the adsorbent and flushed with pure water at a constant flow rate. The adsorption experiments were performed at the same flow rate by using a set of solutions containing sequentially increasing surfactant concentrations. The concentration fronts passing through the column were monitored continuously by the RID connected to the exit port of the calorimeter. For a small concentration step, the amount adsorbed $\delta\Gamma$ is related to the retention time and can be calculated from the breakthrough curve.[15,18] The associated enthalpy of adsorption $\delta_{ads}H$ appears as a calorimetric peak. Thus, the differential enthalpy of adsorption is directly measured as $\Delta_{ads}h = \delta_{ads}H/\delta\Gamma$ for each step. Typical instrumental response curves are displayed in Figure 1. The adsorption process was found to be reversible for the C_nTAB with $n = 6$, 8, and 10. For $C_{12}TAB$, the desorption steps were slow compared with the adsorption steps. Strongly elongated breakthrough curves and heavy tailing of the calorimeter peaks were observed in the submonolayer region when the concentration was successively decreased to zero. For the C_{14} and C_{16} surfactants, effectively irreversible adsorption steps were experienced over a wide range of surface coverage: once the surfactant molecules were bound to the surface, the adsorption layer remained stable even in a stream of pure water. However, the graphite surface was easily regenerated when the column was flushed with an aqueous butanol solution and then with pure water.

High-affinity adsorption may impose severe limitations on the application of the frontal-flow method. When the surface becomes saturated at equilibrium concentrations near the detection limit of the RID, and for nonreversible adsorption in general, monolayer formation cannot be resolved with adequate accuracy. To overcome such difficulties for chain lengths $n > 12$, we used another method designed for the study of nonreversible adsorption processes at solid/liquid interfaces.

Pulsed-Flow Calorimetry. The experimental setup is only slightly different from that of frontal-flow calorimetry. A permanent flow of water is maintained throughout the column. At the input port of the calorimeter, known amounts of a surfactant solution are injected into the column in a series of small pulses, with time intervals sufficient for thermal equilibrium to be attained between them. For nonreversible adsorption, the solid surface is successively saturated in this way. For each injection, the amount of surfactant adsorbed $\delta\Gamma$ is calculated by taking the difference in the RID peak area of the input pulse and the output pulse. The input peak is conveniently measured in a separate blank experiment, in the absence of the adsorbent (calibration peak). In addition to $\delta\Gamma$, the associated heat effect $\delta_{ads}H$ is simultaneously measured for each pulse. Hence, the differential enthalpy of adsorption is given by $\Delta_{ads}h = \delta_{ads}H/\delta\Gamma$. Typical instrumental response curves are displayed in Figure 2.

It may be inferred from the shape of the RID signal that physisorption in the classical sense does not occur: the small peaks recorded on the output solution represent surfactant molecules passing through the loosely packed column without contact with the adsorbent bed. For $n = 12$, Figure 3 depicts a good agreement between the calorimetric data obtained by the two complementary techniques. The pulsed-flow method could not be applied for the C_nTABs with $n < 12$ (reversible adsorption), and the resolution of the frontal-flow method was not satisfactory for $n > 12$ (high-affinity adsorption). A detailed analysis of the calorimeter signal and the RID signal for reversible adsorption, nonreversible adsorption, and a combination of the two cases will be discussed elsewhere.

Thermodynamic Considerations. The nominal (but hypothetical) range of surface concentration of C_nTAB for $n = 6-16$ in a close-packed monolayer on graphite can be estimated by using a geometric model of epitaxial ordering[15] as 2.65−1.45 $\mu mol \cdot m^{-2}$. Figure 3 depicts the differential enthalpies of adsorption in the submonolayer region at 298.15 K, before the surface is sufficiently preconcentrated to induce hemimicellization.[14−16] $\Delta_{ads}h$ appears to be independent of the surface composition, as an indication of the ideal behavior of the adsorption layer in this region. This behavior can be explained

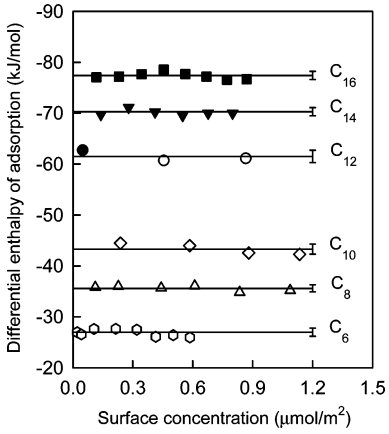

Figure 3. Differential molar enthalpies plotted against surface concentration in the submonolayer region. Adsorption of C_nTAB ($n = 6-16$) from aqueous solutions onto graphite at 298.15 K. Open symbols: frontal-flow calorimetry. Solid symbols: pulsed-flow calorimetry.

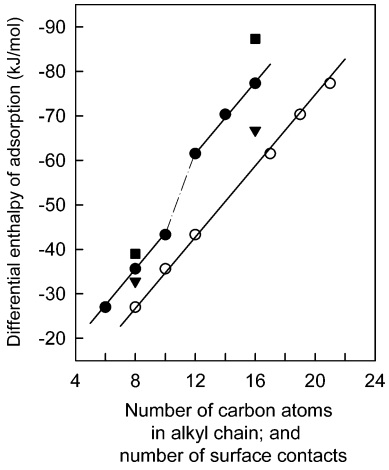

Figure 4. Differential molar enthalpies of the monolayer formation of C_nTAB at the graphite/water interface in two different representations. Solid symbols: plotted against the number of carbon atoms in the alkyl chain. Open symbols: plotted against the number of surface contacts postulated in Figure 5. 288.15 K (▼); 298.15 K (●, ○); 318.15 K (■).

in terms of the coexistence of two monolayer phases, consisting of pure water and essentially pure surfactant, respectively. We propose that at the beginning of the adsorption process, isolated surfactant molecules are adsorbed in their all-trans zigzag conformation along one of the three axes of symmetry of the graphite basal planes. These adsorbate molecules serve as nuclei for 2D crystallization on the surface via growth in epitaxially ordered domains in which the surfactant molecules assemble parallel to each other and in a head-to-head, tail-to-tail orientation. This adsorption mechanism is consistent with AFM images at a later stage of the adsorption process, because surface hemicylinders, templated by the ordered monolayer, were observed only in three domain orientations at 120° to each other and at right angles to the substrate symmetry axes, and the repeat spacing in a single domain was slightly more than twice the length of a fully extended surfactant molecule.[5−13] Monolayer formation is an exothermic process, and the enthalpy of adsorption increases with the carbon number n of the hydrocarbon chain as illustrated in Figure 4. The relationship is markedly linear for $n = 6-10$, and for $n = 12-16$, apparently with the same slope of $-\delta H_n = -\delta(\Delta_{ads}h)/\delta n = 4.0 \pm 0.1$ kJ/(mol n) in the two respective regions. There is a break in the intermediate region between $n = 10$ and $n = 12$, where the

Figure 5. Proposed conformations for the epitaxial adsorption of C_n-TAB molecules from aqueous solutions onto graphite below and above the critical chain length. (A) $n \leq 10$; (B) $n \geq 12$.

enthalpy increment is increased ca. 2.5-fold. If this higher increase in $-\delta H_n$ originates from the appearance of additional lateral interactions between the adsorbed alkyl chains, one would expect a steady increase in $-\Delta_{ads}h$ with a similar slope for $n \geq 10$, but this is not justified by Figure 4. We offer two alternative explanations for this anomaly connected with a characteristic value of n, called here the critical chain length (ccl): a change in the headgroup orientation at the ccl, or the formation of different 2D crystal structures below and above the ccl. These two cases may also be mutually interrelated.

Discussion

Change in the Headgroup Orientation at the ccl. We measured the adsorption isotherm of tetramethylammonium bromide at the graphite/water interface at 298.15 K. The adsorption of this electrolyte at low concentrations proved to be slightly negative with respect to water. Therefore, as the ionic character of C_nTAB increases with decreasing n, the headgroup is likely to be lifted away from the surface, with the anchor chain remaining adsorbed. On the other hand, the hydrophobic character of C_nTAB increases with increasing n, and (partial) association of the ammonium ions with bromide ions would therefore facilitate the adsorption of the methyl groups of the ammonium head. It appears adequate to assume that the headgroup is exposed to the aqueous phase below the ccl ($n \leq 10$), and the adsorption is therefore reversible in this case. Further, the headgroup is bound to the surface above the ccl ($n \geq 12$), and the adsorption tends to become nonreversible with increasing n. We suggest that, within a homologous surfactant series, the ccl and δH_n at the ccl are characteristics of the particular headgroup. Additionally, for the special case of the trimethylammonium head, we found a correlation between n and the number of *effective* surface contacts m.

Figure 5 depicts two of the few plausible conformations (obtained from Dreiding models) below and above the ccl, respectively, which are consistent with the calorimetric data in Figure 4. For C_nTAB with $n \leq 10$, two H atoms of the *C*-methyl group, two H atoms of the methylene group adjacent to the ammonium head, and one H atom of each of the other methylene groups are in contact with the surface. The three *N*-methyl groups are exposed to the aqueous phase, with no contact with the surface (Figure 5). The total number of surface contacts is then $m = n + 2$. For C_nTAB with $n \geq 12$, two H atoms of the *C*-methyl group, one H atom of each of the methylene groups, and 2×2 H atoms of two *N*-methyl groups are in contact with the surface; the third *N*-methyl group is directed toward the aqueous phase (Figure 5). Thus, $m = n + 5$. The plot of $\Delta_{ads}h$ against m is included in Figure 4. This representation yields a straight line throughout the range $m = 8-21$, with a slope of $-\delta H_m = -\delta(\Delta_{ads}h)/\delta m = 4.0$ kJ/(mol m) to a very good approximation. We conclude, therefore, that the observed break in $\Delta_{ads}h$ vs n is consistent with the picture of headgroup

reorientation as the ccl is reached; i.e., the headgroup changes from nonbonding to bonding with respect to the surface. C_nTAB with $n = 12$, 14, and 16 forms hemicylindrical aggregates on the top of the underlying monolayer.[6−9,15] Previous AFM measurements of nonionic surfactants adsorbed to graphite suggested that the degree of surface-induced ordering below a critical alkyl length is insufficient to template the growth of hemicylindrical hemimicelles.[12,13] Whether $C_{10}TAB$ forms surface hemicylinders remains to be seen. Nonreversible adsorption at the graphite/water interface has already been reported for surfactants with different chain lengths and headgroups.[13−17] Further systematic investigations would be needed to clarify the ccl and the δH_n dependences of various homologous surfactant series on the nature of the headgroup, and to elucidate the headgroup reorientation in terms of the enthalpy/entropy balance of the process.

Different 2D Crystal Structures Below and Above the ccl. It was argued in a recent AFM study that the first layer of C_{16}-TAB molecules on the surface of graphite does not represent a cut through any orientation of the three-dimensional (3D) crystal: the adsorbed layer has a period mismatch or an orientational mismatch, so the graphite templates the formation of an alternative structure and inhibits the formation of the bulk crystalline structure.[9] Nevertheless, we can provide supporting evidence of the close *similarity* between surface-directed ordering and 3D crystallization in the bulk. X-ray diffraction studies on the 3D bulk crystal structure of long-chain alkylammonium halides, including bromides, revealed that the room temperature forms are tetragonal up to $n = 10$, and monoclinic for $n = 12-16$.[21,22] Differential scanning calorimetry studies revealed the occurrence of several phase transformations for these compounds.[21,22] For instance, a solid/solid phase transition far below the melting points of 3D crystals of C_nTABs was attributed to freezing/melting of the layer of hydrocarbon chains, the rigid ionic layer being retained in the regular arrangement.[22] The enthalpy of this transition exhibited a jump between $n = 10$ and $n = 12$, i.e., at the same chain length as that for which the crystal structure changes from tetragonal to monoclinic. This is in nominal agreement with the ccl observed in the present work. Further, we measured the enthalpies of adsorption of C_8-TAB and $C_{16}TAB$ at three different temperatures; the results are given in Figure 4. Although monolayer formation displays a normal temperature dependence, the process becomes more exothermic as the temperature is raised from 288.15 to 318.15 K. Hence, the heat capacity of monolayer formation is negative, and the longer the chain, the larger this heat capacity is. For comparison, the molar enthalpy of the transfer of $C_{16}TAB$ molecules from a dilute aqueous solution to a pure, 3D crystalline phase[23] is ca. 10 kJ/mol less negative than the transfer into a 2D array on the surface of graphite, over the same range of temperature as in the present study. A similar trend holds for the crystallization of $C_{10}TAB$ at 298.15 K.[24] These enthalpy data and the similar heat capacities provide further calorimetric evidence that surface-directed ordering may be regarded as 2D crystallization. Besides the interplay of surface−molecule and molecule−molecule interactions in the 2D phase, dehydration of the surfactant molecules when they are transferred from the aqueous phase to the surface represents a very important contribution to the overall enthalpy change.

Future Perspectives of Pulsed-Flow Calorimetry. The above results demonstrate that liquid-flow calorimetry is a sensitive tool for elucidation of the thermodynamic aspects of surface-directed ordering. Further, the pulsed-flow method may open up new perspectives in thermodynamic and structural investigations of nonreversible phenomena at solid/solution interfaces. Among others, the high-affinity adsorption of other surfactants, the high-affinity adsorption of macromolecules, and specific ion adsorption on ion-exchanger supports can be studied by means of this method. As concerns the potential applications, catalytic and other interfacial reactions performed directly in the calorimeter vessel, and the surface characterization of heterogeneous catalysts by the chemisorption of suitably selected probe molecules from inert solvents (for mapping surface energy distribution), seem to be particularly promising.

Summary

We applied frontal-flow and pulsed-flow calorimetric methods to study the monolayer formation of even-numbered alkyltrimethylammonium bromides C_nTAB ($n = 6-16$) at the graphite/water interface. We showed the following: (i) the differential heat of adsorption ($-\Delta_{ads}h$) is independent of the surface coverage; (ii) pure water and pure surfactant domains coexist in the submonolayer region; (iii) the adsorption is more exothermic at higher temperature; (iv) $-\Delta_{ads}h$ is a linear function of the number n of carbon atoms in the alkyl chain; (v) this linear relationship has a step at a critical chain length (ccl); (vi) the adsorption becomes nonreversible above the ccl; (vii) a reorientation of the headgroup occurs at the ccl; (viii) $-\Delta_{ads}h$ is a linear function of the number m of effective surface contacts; (ix) monolayer formation may be regarded as 2D crystallization; (x) different crystal structures exist below and above the ccl; (xi) the degree of surface-induced ordering below the ccl may be insufficient to template the formation of surface hemicylinders.

It is anticipated that pulsed-flow calorimetry has a high potential for investigations of nonreversible solid/liquid interfacial phenomena in a variety of disciplines in chemistry.

Acknowledgment. This work was supported by a research fellowship from the Alexander von Humboldt Foundation (Z.K.), by the Hungarian Scientific Research Fund (OTKA T042521 and T047390), and by the German Research Foundation (DFG) through SFB 448.

References and Notes

(1) Rabe, J. P.; Buchholz, S. *Science* **1991**, *253*, 242−427.

(2) Cyr, D. M.; Venkataraman, B.; Flynn, G. W. *Chem. Mater*. **1996**, *8*, 1600−1615.

(3) Kern, H. E.; Findenegg, G. H. *J. Colloid Interface Sci.* **1980**, *75*, 346−356.

(4) Liphard, M.; Glanz, P.; Pilarski, G.; Findenegg, G. H. *Prog. Colloid Polym. Sci.* **1980**, *67*, 131−140.

(5) Wanless, E. J.; Ducker, W. A. *J. Phys. Chem.* **1996**, *100*, 3207−3214.

(6) Manne, S.; Cleveland, J. P.; Gaub, H. E.; Stucky, G. D.; Hansma, P. K. *Langmuir* **1994**, *10*, 4409−4413.

(7) Manne, S.; Gaub, H. E. *Science* **1995**, *270*, 1480−1482.

(8) Manne, S. *Prog. Colloid Polym. Sci.* **1997**, *103*, 2226−2233.

(9) Liu, J.-F.; Ducker, W. A. *J. Phys. Chem. B* **1999**, *103*, 8558−8567.

(10) Kawasaki, H.; Syuto, M.; Maeda, H. *Langmuir* **2001**, *17*, 8210−8213.

(11) Patrick, H. N.; Warr, G. G.; Manne, S.; Aksay, I. A. *Langmuir* **1997**, *13*, 4349−4356.

(12) Grant, L. N.; Tiberg, F.; Ducker, W. A. *J. Phys. Chem. B* **1998**, *102*, 4288−4294.

(13) Holland, N. B.; Ruegsegger, M.; Marchant, R. E. *Langmuir* **1998**, *14*, 4, 2790−2795.

(14) Király, Z.; Findenegg, G. H.; Klumpp, E.; Schlimper, H.; Dékány, I. *Langmuir* **2001**, *17*, 2420−2425.

(15) Király, Z.; Findenegg, G. H. *J. Phys. Chem. B* **1998**, *102*, 1203−1211.

(16) Király, Z.; Findenegg, G. H. *Langmuir* **2000**, *16*, 8842−8849.
(17) Findenegg, G. H.; Pasucha, B.; Strunk, H. *Colloids Surf.* **1989**, *37*, 223−233.
(18) Király, Z. In *Thermal Behavior of Dispersed Systems*; Garti, N., Ed.; Marcel Dekker: New York and Basel, 2001; pp 335−356.
(19) Groszek, A. J. *Nature* **1958**, *182*, 1152−1153.
(20) Groszek, A. J. *Stud. Surf. Sci. Catal.* **1999**, *120A*, 143−175.
(21) Tsau, J.; Gilson, D. F. R. *J. Phys. Chem.* **1968**, *72*, 4082−4085.
(22) Iwamoto, K.; Ohnuki, Y.; Sawada, K.; Seno, M. *Mol. Cryst. Liq. Cryst.* **1981**, *73*, 95−103.
(23) Bergström, S.; Olofsson, G. *Thermochim. Acta* **1986**, *109*, 155−164.
(24) Bury, R.; Mayaffre, A.; Treiner, C. *J. Chem. Soc., Faraday Trans. 1* **1983**, *79*, 2517−2528.